PHYSICAL REVIEW B **71**, 064205 (2005)

# Fast dynamics of $H_2O$ in hydrous aluminosilicate glasses studied with quasielastic neutron scattering

Sylvio Indris* and Paul Heitjans†
*Institut für Physikalische Chemie und Elektrochemie, Universität Hannover, Callinstraße 3-3A, D-30167 Hannover, Germany*

Harald Behrens
*Institut für Mineralogie, Universität Hannover, Callinstraße 3, D-30167 Hannover, Germany*

Reiner Zorn
*Institut für Festkörperforschung, Forschungszentrum Jülich GmbH, D-52425 Jülich, Germany*

Bernhard Frick
*Institut Laue-Langevin, 6 rue Jules Horowitz, F-38042 Grenoble, Cedex 9, France*

(Received 14 July 2004; published 25 February 2005)

We studied the dynamics of dissolved water in aluminosilicate glasses with the compositions $NaAlSi_3O_8 \cdot 0.3H_2O$, $NaAlSi_3O_8 \cdot 1.3H_2O$ and $Ca_{0.5}AlSi_3O_8 \cdot 1.3H_2O$ using quasielastic neutron scattering. As shown by near-infrared spectroscopy on these samples, $H_2O$ molecules are the predominant hydrous species in the water-rich glasses whereas OH groups bound to tetrahedrally coordinated cations are predominant at low water contents. Backscattering and time-of-flight methods were combined to investigate motional correlation times in the range between 0.2 ps and 2 ns. For the water-rich glasses an elastic scan between 2 K and 420 K shows that the dynamical processes set in at lower temperatures in the Ca-bearing glass than in the Na-bearing glass. This is corroborated by the broadening of the inelastic spectra $S(Q,\omega)$. The shape of the scattering function $S(Q,t)$ suggests a distribution of activation barriers for the motion of hydrous species in the disordered structure of the glass. The distribution is narrower and the average activation energy is smaller in the Ca-bearing glass than in the Na-bearing glass. No indication for dynamics of hydrous species was found at temperatures up to 520 K in the water-poor glass $NaAlSi_3O_8 \cdot 0.3H_2O$ containing dissolved water mainly in the form of OH groups. It is concluded that $H_2O$ molecules are the dynamic species in the above-mentioned time regime in the water-rich glasses. The dynamic process is probably a rotation of $H_2O$ molecules around their bisector axis.

DOI: 10.1103/PhysRevB.71.064205 PACS number(s): 61.12.−q, 61.43.Fs, 66.30.−h, 93.85.+q

## I. INTRODUCTION

Knowledge of dynamic processes of hydrous species in silicate glasses is important in geosciences and materials science, e.g., for understanding and modeling of processes during volcanic eruptions and corrosion of glass. Glasses produced by quenching silicate melts at ambient pressure contain usually not more than a few hundreds to thousands of ppm by weight of $H_2O$. Nevertheless, these small quantities of dissolved water can have large effects on physical and chemical properties of the glasses, e.g., lowering the glass transition temperature by several tens to hundreds of kelvin[1–3] and decreasing strongly the optical transmittance in the mid-infrared.[4] Larger amounts of dissolved $H_2O$ of up to 8 wt. % are found in natural glasses of volcanic origin, either in small quantities as glass inclusions in minerals[5] or as extended rocks such as pitchstone.[6] Water-rich layers containing sometimes more than 10 wt. % $H_2O$ can be formed by corrosion of glasses. Such hydration layers have been used for dating obsidian artifacts.[7] In the laboratory up to 20 wt. % $H_2O$ can be incorporated in silicate glasses by fusion of glass powder and $H_2O$ at high pressure.[8,9]

As shown by near-infrared (NIR) and nuclear magnetic resonance (NMR) spectroscopy, water dissolves in silicate glasses and melts in the form of at least two different species, OH groups and $H_2O$ molecules.[4,8,10–13] Figure 1 shows a sketch of the structure of hydrous alkali and alkaline earth aluminosilicate glasses. In these glasses aluminium is incorporated on tetrahedral sites with its charge being compensated by $Na^+$ or $Ca^{2+}$. $SiO_4$ and $AlO_4$ tetrahedra form a completely polymerized three dimensional network. Introducing water as OH groups leads to disruption of oxygen bridges and thus to a softening of the network while molecular water leaves the network unchanged. For low water contents OH groups are the dominant hydrous species in glasses, but with increasing water content $H_2O$ molecules become more abundant whereas the OH concentration reaches a constant level.[4,8,14,15]

Information on the dynamics of hydrous species in silicate glasses is available for elevated temperatures from studies on water diffusion, electrical conductivity, internal friction and water speciation. Much less is known about motions of such species at low temperatures. NMR observations indicate that rotation of $H_2O$ molecules around their bisector axis can be activated in alkali aluminosilicate glasses already at temperatures around 140 K but details of this motional process are unknown.[12,13,16,17] In this paper we have investigated the dynamics of hydrous species in silicate glasses at temperatures

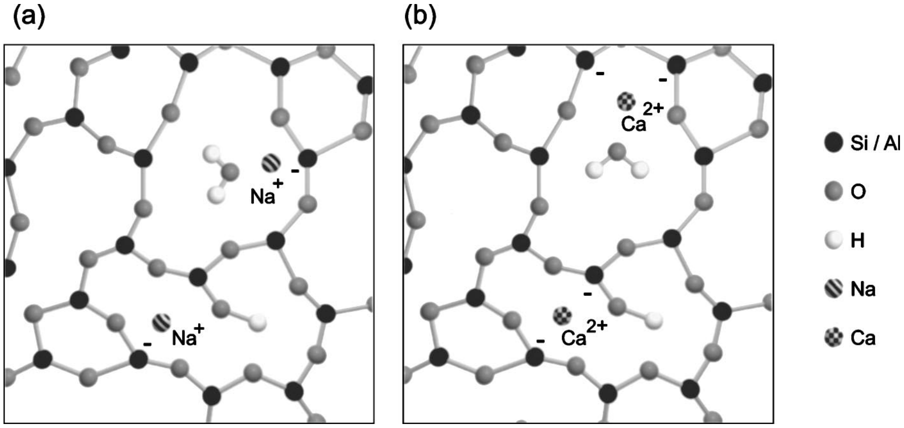

FIG. 1. Sketch of the structure of (a) an alkali and (b) an alkaline-earth aluminosilicate glass containing water in molecular form and as OH groups. The excess charge of tetrahedrally coordinated aluminium ($AlO_4^-$, marked with a minus sign) is balanced by alkali and alkaline-earth ions, respectively. For the sake of clarity, in this two-dimensional plot the Si as well as the Al atoms are drawn as threefold coordinated.

ranging from 2 K to 423 K using incoherent quasielastic neutron scattering. Combining neutron time-of-flight and backscattering spectroscopy, motional correlation times[37] in the range from 0.2 ps to 2 ns are covered. For a detailed description of these methods see, e.g., Refs. 18 and 19. Measurements were performed on two hydrated glasses with the anhydrous compositions $NaAlSi_3O_8$ and $Ca_{0.5}AlSi_3O_8$ which show a large difference in bulk water diffusivity $D_{\mathrm{water}}$. At 1 wt. % water content (corresponding to the compositions $NaAlSi_3O_8 \cdot 0.15H_2O$ and $Ca_{0.5}AlSi_3O_8 \cdot 0.15H_2O$, respectively) and $T = 870$ K, $D_{\mathrm{water}}$ is about two orders of magnitude greater in the Na-bearing than in the Ca-bearing glass ($8.9 \times 10^{-14}$ m$^2$/s and $5.7 \times 10^{-16}$ m$^2$/s, respectively[20]). It was suggested that the slower water diffusion in the Ca-bearing glass is due to binding of $H_2O$ molecules in strong complexes with $Ca^{2+}$, and to the strengthening of the glass structure by incorporation of divalent cations. It is one of the objectives of this study to get new insights into the dynamics of hydrous species in silicate glasses and into the effect of different cations on motional processes of $H_2O$ molecules, OH groups and protons.

## II. SYNTHESIS AND CHARACTERIZATION OF HYDROUS GLASSES

Hydrous glasses were produced by fusion of glass powder and bidistilled $H_2O$ in an internally heated gas pressure vessel at 1523 K and 500 MPa. The samples we studied are $NaAlSi_3O_8 \cdot 0.3H_2O$ labeled in this paper as Ab2, $NaAlSi_3O_8 \cdot 1.3H_2O$ (Ab8), and $Ca_{0.5}AlSi_3O_8 \cdot 1.3H_2O$ (AQ8). The labels were derived from the minerals' names albite ($NaAlSi_3O_8$) and anorthite/quartz ($CaAl_2Si_2O_8/SiO_2$). The numbers in the labels denote the $H_2O$ contents in wt. %. A list of the samples and some characteristics are given in Table I. The two water-rich samples contain ≈24 mol % (8 wt. %) dissolved $H_2O$ whereas $NaAlSi_3O_8 \cdot 0.3H_2O$ con-

TABLE I. Sample characterization and IR spectroscopic data. The density of $NaAlSi_3O_8 \cdot 0.3H_2O$ and $NaAlSi_3O_8 \cdot 1.3H_2O$ was calculated according to Ref. 21 and the density of $Ca_{0.5}AlSi_3O_8 \cdot 1.3H_2O$ was calculated according to Ref. 22. The thickness is an average value for all wafers of the respective composition. Contents of water dissolved as OH and as $H_2O$ were determined from the peak height of the IR absorption bands at 4500 cm$^{-1}$ and 5200 cm$^{-1}$, respectively. The reported water contents are average values based on 8 to 16 spectra which were recorded on six or more glass plates. The water contents in mol % refer to the composition of oxides, e.g., 9.5 mol % $Na_2O$ – 9.5 mol % $Al_2O_3$ – 57 mol % $SiO_2$ – 24 mol % $H_2O$ for Ab8.

| Sample | Ab2 | Ab8 | AQ8 |
|---|---|---|---|
| Anhydrous composition | $NaAlSi_3O_8$ | $NaAlSi_3O_8$ | $Ca_{0.5}AlSi_3O_8$ |
| Hydrous composition | $NaAlSi_3O_8 \cdot 0.3H_2O$ | $NaAlSi_3O_8 \cdot 1.3H_2O$ | $Ca_{0.5}AlSi_3O_8 \cdot 1.3H_2O$ |
| | ($NaAlSi_3O_8$ + 7 mol % $H_2O$) | ($NaAlSi_3O_8$ + 24 mol % $H_2O$) | ($Ca_{0.5}AlSi_3O_8$ + 24 mol % $H_2O$) |
| | ($NaAlSi_3O_8$ + 2 wt. % $H_2O$) | ($NaAlSi_3O_8$ + 8 wt. % $H_2O$) | ($Ca_{0.5}AlSi_3O_8$ + 8 wt. % $H_2O$) |
| Density in g/cm$^3$ | 2.356 | 2.274 | 2.326 |
| Thickness in mm | 0.982 | 0.769 | 0.775 |
| Water content in mol % | | *after synthesis* | |
| as OH | 4.6 ± 0.1 | 5.8 ± 0.1 | 6.3 ± 0.1 |
| as $H_2O$ | 2.3 ± 0.2 | 18.2 ± 0.5 | 17.8 ± 0.7 |
| total | 6.9 ± 0.3 | 24.0 ± 0.5 | 24.1 ± 0.7 |
| Water content in mol % | | *after experiment* | |
| as OH | 4.6 ± 0.1 | 5.8 ± 0.1 | 6.5 ± 0.1 |
| as $H_2O$ | 2.2 ± 0.2 | 18.0 ± 0.4 | 17.2 ± 0.3 |
| total | 6.8 ± 0.3 | 23.8 ± 0.4 | 23.7 ± 0.5 |

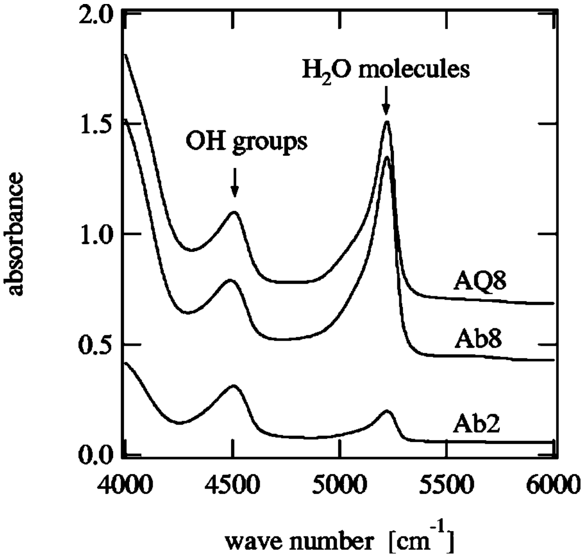

FIG. 2. Near-infrared absorption spectra of $NaAlSi_3O_8 \cdot 0.3H_2O$ (Ab2), $NaAlSi_3O_8 \cdot 1.3H_2O$ (Ab8) and $Ca_{0.5}AlSi_3O_8 \cdot 1.3H_2O$ (AQ8) recorded after the neutron scattering experiments. The absorbance is normalized to a sample thickness of 1 mm in each case. For clarity, the spectra of Ab8 and AQ8 are plotted with an offset of 0.3 and 0.6, respectively.

tains only 7 mol % (2 wt. %) dissolved $H_2O$. The water contents given in mol % refer to the composition of oxides. To fill the large area of the sample holder used for neutron scattering six capsules (platinum, size: $30 \times 10 \times 2$ mm$^3$, wall thickness 0.2 mm) were prepared for each composition. All samples for each composition were processed in a single experiment to ensure identical synthesis conditions. Capsules were quenched isobarically with an initial cooling rate of ca. 200 K/min decreasing to ca. 100 K/min in the range of glass transition (between 600 K and 900 K), which depends on water content and anhydrous composition.[3]

Glass plates were doubly polished and analyzed by IR spectroscopy to determine the concentrations of OH groups and $H_2O$ molecules and to test the homogeneity of hydrous species in the glasses. The wafers were mounted on a hole aperture 2 mm in diameter and spectra were recorded with an FTIR spectrometer Bruker IFS88 using a tungsten light source, a $CaF_2$ beamsplitter, and an InSb detector. 100 scans were accumulated for each spectrum with a spectral resolution of 4 cm$^{-1}$. Three to four spectra were recorded on each glass plate before and after the neutron scattering experiments.

Near-infrared absorption spectra of the three glasses are shown in Fig. 2. The bands near 4500 cm$^{-1}$ and near 5200 cm$^{-1}$ are attributed to combination modes of OH groups and $H_2O$ molecules, respectively.[4,10] Concentrations of both species were determined from the peak heights of the bands after subtracting a linear baseline fitted to the 5200 cm$^{-1}$ band and extended to the 4500 cm$^{-1}$ band (GG-type baseline[21]). Species concentrations were calculated by Lambert-Beer's law

$$c_i = \frac{A_i}{d\,\varepsilon_i}, \quad (1)$$

where i refers to the species OH and $H_2O$ and their corresponding absorption bands at 4500 and 5200 cm$^{-1}$, respectively. $c_i$ is the concentration of water dissolved as species i, $A_i$ is the absorbance of the combination band related to species i, $d$ is the sample thickness, and $\varepsilon_i$ is the molar absorption coefficient. Calibrations of $\varepsilon$ values and density-water content relationships have been performed earlier, separately for the Na and the Ca glasses.[8,22]

In the water-rich glasses $NaAlSi_3O_8 \cdot 1.3H_2O$ and $Ca_{0.5}AlSi_3O_8 \cdot 1.3H_2O$ molecular $H_2O$ is the dominant species and only 1/4 of the dissolved water is dissociated to OH groups. In contrast, molecular $H_2O$ is a minor species in $NaAlSi_3O_8 \cdot 0.3H_2O$ with a relative abundance of only 1/3 (Table I). After the IN10 experiment in which the sample was finally heated to 423 K, the sample of $NaAlSi_3O_8 \cdot 1.3H_2O$ was pale due to numerous cracks. We attribute the formation of cracks to a spontaneous release of internal stress which is caused by large oversaturation with molecular $H_2O$ (glasses are synthesized at 500 MPa but experiments are performed at ambient pressure). Spontaneous stress release within a few seconds could be observed with a microscope in heating stage experiments with water-rich $NaAlSi_3O_8$ glasses ($>13$ mol % $H_2O$) but not with water-poor glasses ($<13$ mol % $H_2O$). However, the formation of cracks in $NaAlSi_3O_8 \cdot 1.3H_2O$ is not associated with a loss of water or a change in relative abundance of hydrous species. After the final IN6 experiment all glasses contain unchanged concentrations of OH groups and $H_2O$ molecules (Table I).

## III. EXPERIMENTAL SETUP

In this study we used two different spectrometers to perform inelastic neutron scattering, both located at the Institut Laue-Langevin in Grenoble, France.[18] The backscattering spectrometer IN10 has high energy resolution and the time-of-flight spectrometer IN6 gives access to a large energy transfer range. The combination of these two spectrometers allows one to study dynamical processes in a time window of about four decades from 0.2 ps to 2 ns. Corrections of the raw data concerning the background intensity and the detector efficiency were performed using measurements with an empty cell and a vanadium target, respectively. The observed scattering is mainly incoherent from the protons contained in water molecules or OH groups: 79% for the samples containing 24 mol % water ($NaAlSi_3O_8 \cdot 1.3H_2O$ and $Ca_{0.5}AlSi_3O_8 \cdot 1.3H_2O$) but only 52% for $NaAlSi_3O_8 \cdot 0.3H_2O$.

### A. IN10

The backscattering spectrometer IN10 was used with Si-(111) monochromator and analyzer. This corresponds to a neutron wavelength of 6.271 Å and an energy resolution of 0.9 $\mu$eV [full width at half maximum (FWHM)]. Energy selection is done via a Doppler monochromator resulting in an accessible energy transfer range from $-12$ $\mu$eV to $+12$ $\mu$eV and thus in an accessible time range from 150 ps to 2 ns. The

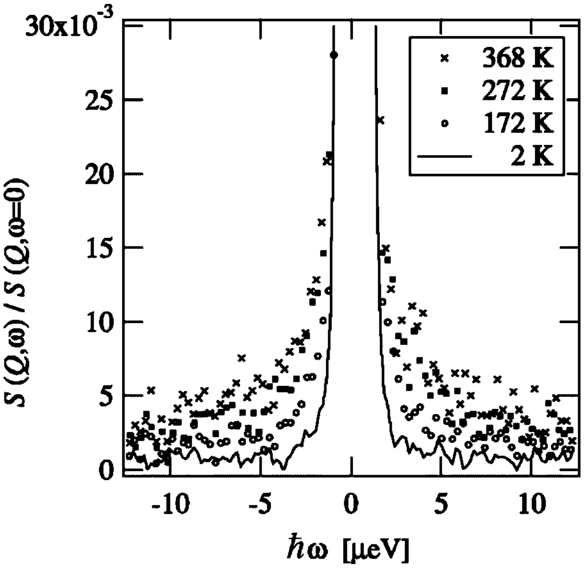

FIG. 3. Normalized neutron backscattering spectra $S(Q,\omega)$ of $NaAlSi_3O_8 \cdot 1.3H_2O$ (Ab8) obtained on IN10. The data of three detectors with $Q=1.68$ Å$^{-1}$, 1.85 Å$^{-1}$, and 1.96 Å$^{-1}$ have been averaged to improve the signal-to-noise ratio.

highest scattering angle was 156° corresponding to a maximum momentum transfer of $Q=1.96$ Å$^{-1}$.

### B. IN6

The time-of-flight spectrometer IN6 was used with an incident wavelength of 5.1 Å resulting in an energy resolution of 100 $\mu$eV (FWHM) and a momentum transfer range from 0.22 Å$^{-1}$ to 2.05 Å$^{-1}$. At $Q=1.85$ Å$^{-1}$ the accessible energy transfer range was −1.15 meV to +15.5 meV due to the kinematic restriction of neutron energy and momentum. From this a dynamic time window from 0.2 ps to 20 ps results after Fourier transform.

## IV. RESULTS

### A. IN10

The inelastic spectra for $NaAlSi_3O_8 \cdot 1.3H_2O$ and $Ca_{0.5}AlSi_3O_8 \cdot 1.3H_2O$ measured at the backscattering spectrometer IN10 are shown in Figs. 3 and 4, respectively, for Q=1.85 Å$^{-1}$ and temperatures between 2 K and 370 K. The spectra for all temperatures are scaled to the same maximum intensity. Although there is a clear quasielastic contribution there is only a minor increase of broadening over the large temperature range on an increasing background due to motions which are too fast to be observed on IN10. This appearance indicates a broad distribution of correlation times of which only a few fall into the dynamic window of backscattering spectroscopy. This in turn is probably due to variations in the local environment of water molecules in these amorphous systems.

The inelastic spectra also show differences between $NaAlSi_3O_8 \cdot 1.3H_2O$ and $Ca_{0.5}AlSi_3O_8 \cdot 1.3H_2O$. Whereas the Na glass exhibits a continuous small increase in line broadening towards higher temperatures in the whole temperature range, for the Ca glass the broadening was observed only at temperatures below 250 K (the spectra at 222 K and 322 K almost coincide; see Fig. 4). An explanation might be a narrower distribution of correlation times for the Ca glass. Hence, all dynamic processes become too fast for the time window of IN10 at temperatures above about 250 K while for the Na glass having a broader distribution always a part of the correlation times falls into the time window of this experiment (see also Sec. IV C).

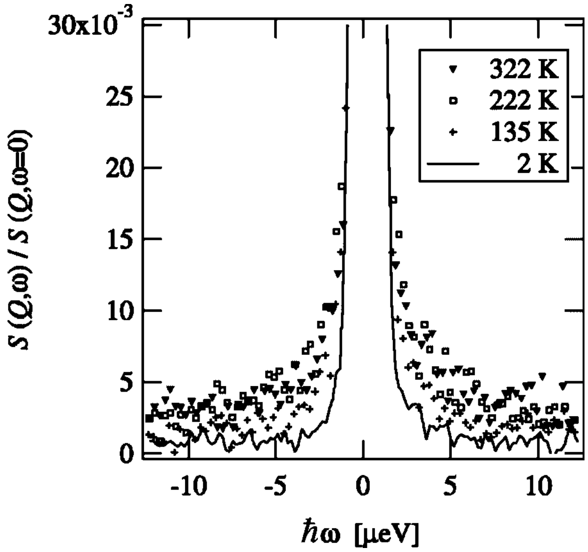

FIG. 4. Normalized neutron backscattering spectra $S(Q,\omega)$ of $Ca_{0.5}AlSi_3O_8 \cdot 1.3H_2O$ (AQ8) obtained on IN10. The data of three detectors with $Q=1.68$ Å$^{-1}$, 1.85 Å$^{-1}$, and 1.96 Å$^{-1}$ have been averaged to improve the signal-to-noise ratio.

We also performed elastic scans in the temperature range from 2 K to 420 K. The height of the elastic peak is decreasing with increasing temperature due to the onset of fast vibrational motions. This is described by the Debye-Waller factor, from which a mean square displacement $\langle u^2 \rangle$ of the dynamic species (in our experiments protons bound in $H_2O$ molecules or OH groups) can be deduced. The temperature dependence of $\langle u^2 \rangle$ is displayed in Fig. 5 for both water-rich samples. (The time scale of $\langle u^2 \rangle$ follows from the resolution of IN10 to be about 1.4 ns. This is significantly larger than any time scale related to vibrations.) The absence of a pronounced step indicates that there is not a single activated process. At temperatures below about 120 K the Debye-Waller factor increases linearly with temperature indicating that vibrational motions are dominating. At higher temperatures one can see a stronger increase of $\langle u^2 \rangle$ which indicates the onset of further dynamical processes. This transition occurs at lower temperatures for the Ca glass (≈120 K) than for the Na glass (≈150 K). Our findings are consistent with NMR results on silicate glasses indicating the onset of twofold rotation of $H_2O$ molecules around their bisector axis with correlation times shorter than $10^{-5}$ s in this temperature range.[12,13] At temperatures above 250 K the slope of $\langle u^2 \rangle$ vs $T$ decreases again for the Ca glass indicating that the dynamical processes become too fast for the time window of IN10 (150 ps−2 ns). This contrasts with the data of the Na

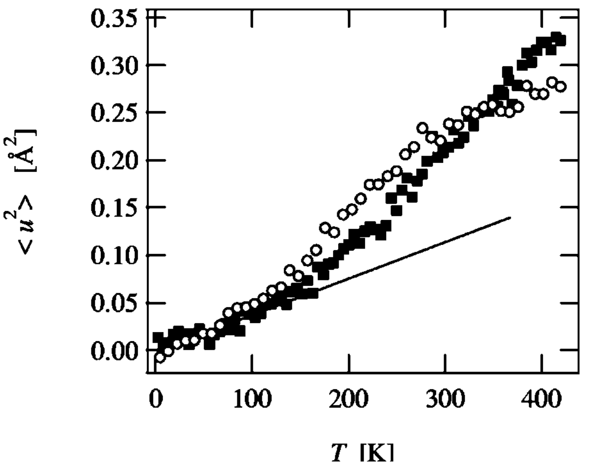

FIG. 5. Mean square displacement $\langle u^2 \rangle$ due to fast motions obtained from elastic scans at IN10 for $NaAlSi_3O_8 \cdot 1.3H_2O$ (■) and $Ca_{0.5}AlSi_3O_8 \cdot 1.3H_2O$ (○). The solid line indicates the linear increase of $\langle u^2 \rangle$ at low temperatures.

glass where a significant fraction of the dynamics is visible up to the highest temperatures. These observations are consistent with the results from the inelastic spectra.

### B. IN6

The inelastic spectra for $NaAlSi_3O_8 \cdot 1.3H_2O$ and $Ca_{0.5}AlSi_3O_8 \cdot 1.3H_2O$ recorded on IN6 are shown in Figs. 6 and 7 for a momentum transfer of 1.85 Å$^{-1}$ and temperatures between 2 K and 370 K. After scaling the maxima of the elastic peaks to the same height, a continuous quasielastic broadening at the bottom of the peak with increasing temperature is evident. From the spectra at the lowest temperatures also the presence of the glass-specific low energy excitations (boson peak) around 6 meV can be seen. This indicates that the dynamics of the hydrogen, which is the main scatterer in these samples, is not fully decoupled from the dynamics of the glass network.

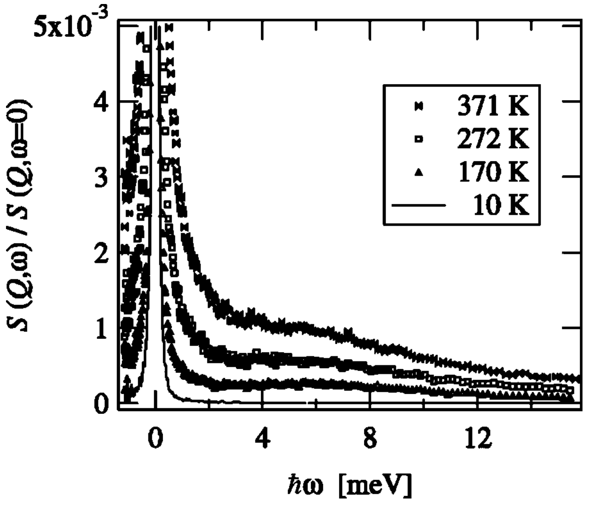

FIG. 6. Normalized neutron time-of-flight spectra $S(Q,\omega)$ of $NaAlSi_3O_8 \cdot 1.3H_2O$ (Ab8) obtained on IN6. Spectra from different detectors have been interpolated to constant $Q$=1.85 Å$^{-1}$.

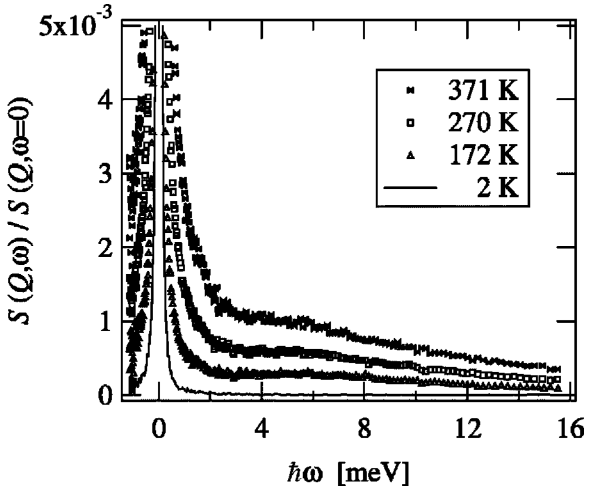

FIG. 7. Normalized neutron time-of-flight spectra $S(Q,\omega)$ of $Ca_{0.5}AlSi_3O_8 \cdot 1.3H_2O$ (AQ8) obtained on IN6. Spectra from different detectors have been interpolated to constant $Q$=1.85 Å$^{-1}$.

For comparison inelastic spectra were also recorded for $NaAlSi_3O_8 \cdot 0.3H_2O$. In this sample, where the water exists mainly in form of OH groups, the quasielastic broadening of the spectra is much weaker, although much higher temperatures (up to 522 K) were applied. This shows that the broadening in the water-rich glasses is caused mainly by the dynamics of molecular $H_2O$.

### C. Time domain analysis

For a quantitative analysis the inelastic scattering data $S(Q,\omega)$ of both spectrometers were Fourier transformed to the time domain and divided by the corresponding resolution data yielding the intermediate scattering function $S(Q,t)$. The results are shown in Figs. 8 and 9 for both water-rich glasses. The combination of the two spectrometers gives an

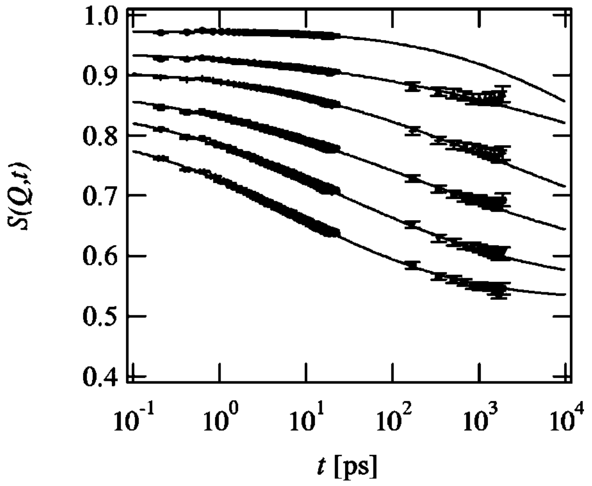

FIG. 8. Incoherent intermediate scattering function $S(Q,t)$ of $NaAlSi_3O_8 \cdot 1.3H_2O$ (Ab8) calculated by Fourier transform of IN6 data (0.2–20 ps) and IN10 data (150–2000 ps), $Q$=1.85 Å$^{-1}$. The different curves belong to temperatures of 99 K, 170 K, 221 K, 272 K, 324 K, and 371 K (top to bottom).

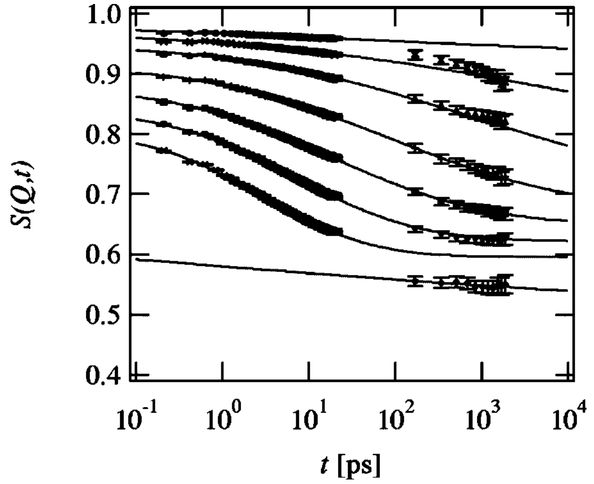

FIG. 9. Incoherent intermediate scattering function $S(Q,t)$ of $Ca_{0.5}AlSi_3O_8 \cdot 1.3H_2O$ (AQ8) calculated by Fourier transform of IN6 data (0.2–20 ps) and IN10 data (150–2000 ps), $Q = 1.85$ Å$^{-1}$. The different curves belong to temperatures of 99 K, 134 K, 172 K, 221 K, 270 K, 321 K, 371 K, and 422 K (top to bottom).

overall accessible time range from 0.2 ps to 2 ns, which is 4 decades. The data from the two experiments, namely from the time-of-flight (0.2 ps–20 ps) and the backscattering spectrometer (150 ps–2 ns) fit together rather well without further scaling factors.

The data can be described in the overall time window 0.2 ps–2 ns by comprising the faster processes into a Debye-Waller factor $A$ and those that are effectively "frozen" on that time scale into an elastic incoherent structure factor EISF yielding

$$S(Q,t) = A\{[1 - \mathrm{EISF}]\phi(t) + \mathrm{EISF}\}, \tag{2}$$

where

$$A = \exp(-\langle u_{\mathrm{fast}}^2\rangle Q^2/3) \tag{3}$$

and

$$\mathrm{EISF} = \exp(-\langle u_{\mathrm{diff}}^2\rangle Q^2/3) \tag{4}$$

describe the $Q$ dependence of $S(Q,t)$. The function $\phi(t)$ describes the time dependence of $S(Q,t)$ and thus the dynamics of the water in the glasses. To fit the experimental data (solid lines in Figs. 8 and 9) we used a log-normal distribution of correlation times[23]

$$g(\ln \tau) = \frac{1}{\sqrt{2\pi}\sigma_{\ln \tau}}\exp\left(-\frac{(\ln \tau - \ln \tau_0)^2}{2\sigma_{\ln \tau}^2}\right) \tag{5}$$

which superimpose to

$$\phi(t) = \int_{\tau=0}^{\infty} \exp(-t/\tau)\, g(\ln \tau)\, \mathrm{d}\ln \tau. \tag{6}$$

The parameters of the log-normal distribution $g(\ln \tau)$ are the average correlation time $\tau_0$ and the width $\sigma_{\ln \tau}$, both being dependent on temperature. This temperature dependence is used in the next subsection to extract the energy barriers for the observed dynamical process.

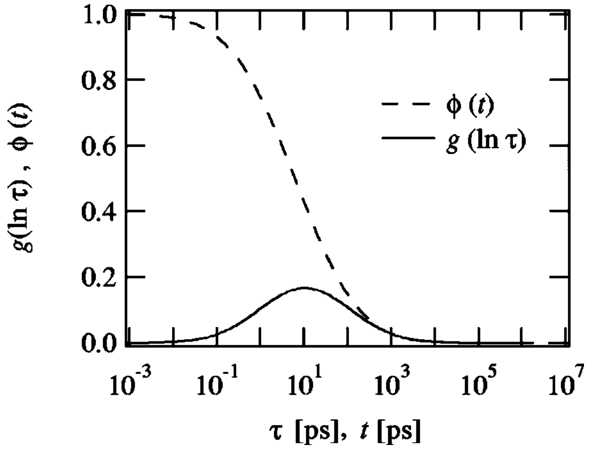

FIG. 10. Log-normal distribution of correlation times $g(\ln \tau)$ and the resulting dynamic function $\phi(t)$ as obtained by fitting Eqs. (2), (6), and (5) to the $S(Q,t)$ data, shown exemplarily for $Ca_{0.5}AlSi_3O_8 \cdot 1.3H_2O$ (AQ8) at 321 K, $Q = 1.85$ Å$^{-1}$.

### D. Energy barrier model

Since the correlation time $\tau$ is expected to show Arrhenius behavior with an activation energy $E_A$,

$$\tau = \tau_\infty \exp(E_A/k_B T), \tag{7}$$

the log-normal distribution of correlation times corresponds to a normal distribution of activation barriers

$$G(E_A) = \frac{1}{\sqrt{2\pi}\sigma_{E_A}}\exp\left(-\frac{(E_A - E_0)^2}{2\sigma_{E_A}^2}\right), \tag{8}$$

which is reasonable due to the amorphous structure of the glasses. The average activation barrier follows from

$$\tau_0 = \tau_\infty \exp(E_0/k_B T). \tag{9}$$

In case that $\tau_\infty$ is constant, i.e., not distributed itself, $\sigma_{\ln \tau}$ and the width of the distribution of activation energies $\sigma_{E_A}$ are related by

$$\sigma_{\ln \tau} = \frac{\sigma_{E_A}}{k_B T}. \tag{10}$$

The results of fitting Eqs. (2), (5), and (6) to the data are shown as solid lines in Figs. 8 and 9 for $NaAlSi_3O_8 \cdot 1.3H_2O$ and $Ca_{0.5}AlSi_3O_8 \cdot 1.3H_2O$, respectively. To get good results for the fit parameters we had to perform global fits of $S(Q,t)$ keeping EISF constant for all temperatures. We get EISF values of $(0.653 \pm 0.008)$ for $NaAlSi_3O_8 \cdot 1.3H_2O$ and $(0.741 \pm 0.004)$ for $Ca_{0.5}AlSi_3O_8 \cdot 1.3H_2O$. Figure 10 shows exemplarily the results for the distribution of correlation times $g(\ln \tau)$ and the resulting $\phi(t)$ [Eq. (6)] for $Ca_{0.5}AlSi_3O_8 \cdot 1.3H_2O$ at 321 K and $Q = 1.85$ Å$^{-1}$. The average correlation times $\tau_0$ are plotted for both water-rich glasses in Fig. 11 vs inverse temperature. Arrhenius behavior is found over a time range of more than 4 decades. The data are fitted with an exponential function according to Eq. (7) to extract the average activation energy $E_0$ from the slope and the preexponential factor $\tau_\infty$ from the ordinate intercept. We obtain $E_0 = (0.27 \pm 0.01)$ eV for $NaAlSi_3O_8 \cdot 1.3H_2O$ and $E_0$

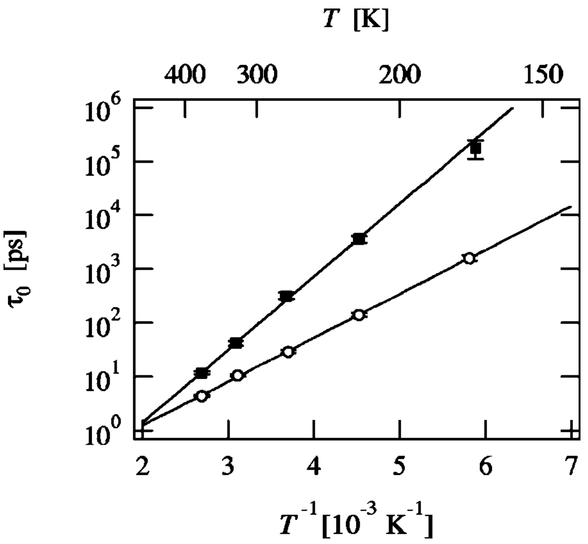

FIG. 11. Average motional correlation times $\tau_0$ obtained from the fit procedure vs inverse temperature for $NaAlSi_3O_8 \cdot 1.3H_2O$ (■) and $Ca_{0.5}AlSi_3O_8 \cdot 1.3H_2O$ (○).

$=(0.16\pm0.01)$ eV for $Ca_{0.5}AlSi_3O_8 \cdot 1.3H_2O$, i.e., a smaller activation energy for the Ca glass. This is consistent with the results from the elastic scan on IN10 (Fig. 5) where the onset of the dynamic process appears at lower temperatures for $Ca_{0.5}AlSi_3O_8 \cdot 1.3H_2O$. The preexponential factor is $\tau_\infty=(2.75\pm0.64)\times10^{-3}$ ps for $NaAlSi_3O_8 \cdot 1.3H_2O$ and $\tau_\infty=(2.91\pm0.32)\times10^{-2}$ ps for $Ca_{0.5}AlSi_3O_8 \cdot 1.3H_2O$. The much smaller $\tau_\infty$ value for the Na glass together with the larger activation energy leads to a crossing of both fitting curves at about 500 K (see Fig. 11). At higher temperatures, which are not accessible for our samples, the dynamics would be faster in the Na glass than in the Ca glass. According to Eq. (8), plotting $\sigma_{\ln\tau}$ vs inverse temperature should give a straight line through the origin if $\tau_\infty$ is constant. As shown in Fig. 12, the data for both, $NaAlSi_3O_8 \cdot 1.3H_2O$ and $Ca_{0.5}AlSi_3O_8 \cdot 1.3H_2O$, can indeed be rather well described by Eq. (8) (though statistical spread for the Na glass is somehow larger). The slopes yield $\sigma_{E_A}=(0.107\pm0.002)$ eV for $NaAlSi_3O_8 \cdot 1.3H_2O$ and $\sigma_{E_A}=(0.069\pm0.001)$ eV for $Ca_{0.5}AlSi_3O_8 \cdot 1.3H_2O$, i.e., the distribution of activation energies is significantly narrower for the Ca glass. This is again in good agreement with the elastic scan on IN10 where the narrow distribution of activation energies and hence correlation times for $Ca_{0.5}AlSi_3O_8 \cdot 1.3H_2O$ passes the experimental time window faster than for $NaAlSi_3O_8 \cdot 1.3H_2O$ where due to the broader distribution always one part of the correlation times falls into the accessible time window. In summary, the results for $E_A$ and $\sigma_{E_A}$ can be used to plot the distributions of activation energies according to Eq. (8) for both glasses; see Fig. 13.

## V. DISCUSSION

### A. Comparison of dynamic processes in glasses

Most of the information on the dynamics of hydrous species in silicate glasses was obtained from water diffusion studies at elevated temperatures, mainly near and above the glass transition temperature. Other sources of information are IR and NMR spectroscopy and electrical conductivity measurements. The basic results and ideas from these studies are summarized in the following section and compared to our results.

Migration of $H_2O$ molecules has been inferred to be the fundamental mechanism for the transport of water in polymerized glasses and melts.[24–29] Two mechanisms were proposed to control the diffusion of $H_2O$ molecules. Several authors suggest that $H_2O$ molecules migrate through the silicate network by direct jumps from one cavity to another, and reaction with oxygen of the silicate network results in an immobilization of the $H_2O$ molecules.[30–32] Another model assumes that the reaction between $H_2O$ molecules and network oxygen forming a pair of OH groups is a transition state during movement of water.[24,25,28,33] The rate-controlling

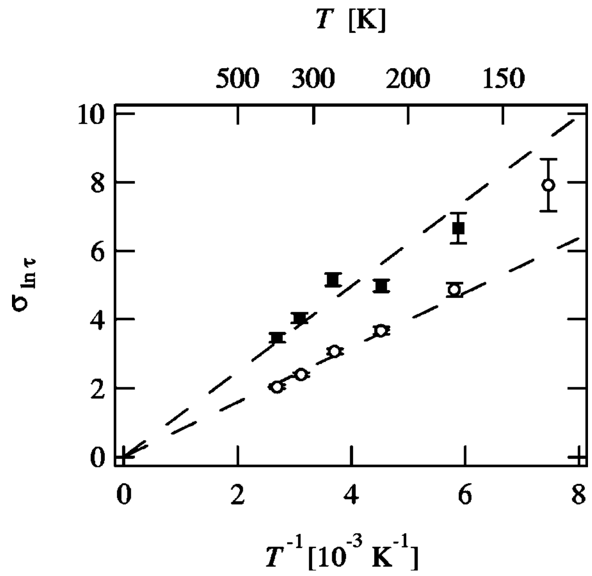

FIG. 12. Width $\sigma_{\ln\tau}$ of the log-normal distribution of motional correlation times vs inverse temperature for $NaAlSi_3O_8 \cdot 1.3H_2O$ (■) and $Ca_{0.5}AlSi_3O_8 \cdot 1.3H_2O$ (○).

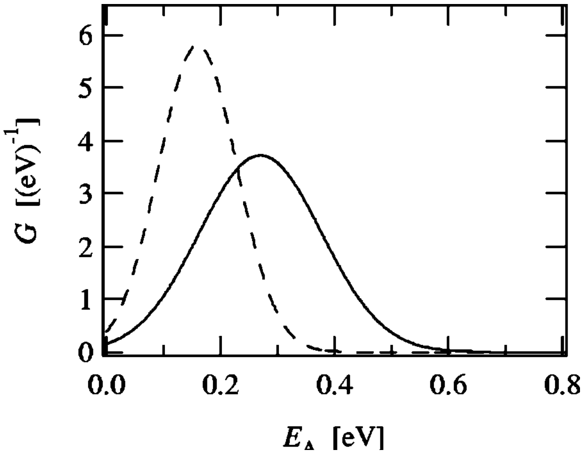

FIG. 13. Normal distribution of activation energies for $NaAlSi_3O_8 \cdot 1.3H_2O$ (Ab8, solid line) and $Ca_{0.5}AlSi_3O_8 \cdot 1.3H_2O$ (AQ8, dashed line).

mechanism may vary with temperature. Above the glass transition, structural relaxation is fast favoring the formation of transient OH group pairs. On the other hand, at low temperatures in the rigid glass structural relaxation is too slow to stabilize the extended transition state required for the formation of OH pairs. Furthermore, at temperatures far below the glass transition the kinetics are too slow to achieve equilibrium for hydrous species. A model for diffusion of water under such nonequilibrium conditions was developed and successfully tested for silica glass by Doremus.[31]

The diffusivity of water is strongly enhanced in aluminosilicate glasses when the alkali content exceeds the quantity required for charge-compensation of aluminium[34] implying that nonbridging oxygen can play an important role in the transport of $H_2O$. Haider and Roberts[34] suggested that coupled motion of $H^+$ and $OH^-$ is a predominant mechanism in depolymerized glasses.

Extrapolated diffusivities of $H_2O$ molecules and protons in silicate glasses are smaller than $10^{-16}\,\mathrm{m^2/s}$ at temperatures below 400 K,[35] corresponding to jump rates smaller than $2\times 10^{-3}\,\mathrm{s^{-1}}$ if a jump distance of 5 Å is assumed. This estimate demonstrates that hopping of hydrous species is too slow to contribute to the dynamic effect observed in our neutron scattering experiments. Another support for this interpretation is given by the higher activation energies for water diffusion [0.6–1.0 eV (Refs. 20, 24, 28, 29, 32, and 34)] and proton conduction [0.9 eV (Ref. 35)] compared to the values found in our neutron scattering study.

Evidence for dynamic processes of hydrous species at low temperatures is given only by NMR spectroscopy. A deuterium NMR study using composite-pulse quadrupolar echo pulse sequences on $D_2O$ bearing rhyolitic glass indicates that a twofold rotation of $D_2O$ around its bisector axis at 173 K is faster than $10^{-5}$ s.[12] In static $^1$H NMR spectra of hydrous alkali aluminosilicate glasses a well resolved Pake doublet (resulting from the strong homonuclear dipole interaction of the two protons in "immobile" water molecules) was observed only at low temperatures around 140 K.[11,13,17,36] This implies that any $H_2O$ motion is frozen in the glasses at these conditions. With increasing temperature the Pake doublet transforms more and more into a single line due to the onset of rotation of $H_2O$ molecules. The motional freedom depends on glass composition, in particular on the $SiO_2$ content. A well resolved Pake doublet could not be observed for very $SiO_2$ rich compositions even at 140 K implying that $H_2O$ molecules have still some motional freedom.[17]

Our neutron scattering data gives access to a more detailed picture of the microscopic processes in water-rich glasses at low temperature because a large temperature range down to 2 K was covered. The results are consistent with the NMR findings that rotation of $H_2O$ molecules in aluminosilicate glasses can be activated at temperatures above 100 K. However, it appears that the motion of $H_2O$ molecules strongly depends on their local environment, as reflected by the broad distribution of activation energies (Fig. 13). Thus the fraction of rotating $H_2O$ molecules continuously increases with temperature and even at the highest temperatures studied a part of the $H_2O$ molecules is probably immobile on the time scale of our experiments.

### B. Structural interpretations

The inelastic spectra as well as the elastic scans on IN10 indicate that the dynamic process probed by neutron scattering is faster in the Ca-bearing glass than in the Na-bearing glass. This is confirmed by the results of the time domain analysis which give shorter average correlation times and a smaller average activation energy for $Ca_{0.5}AlSi_3O_8\cdot 1.3H_2O$. However, the larger preexponential factor $\tau_\infty$ for $Ca_{0.5}AlSi_3O_8\cdot 1.3H_2O$ would lead to an inverted situation at high temperatures. The concentration of low-charged cations ($Na^+$ and $Ca^{2+}$) which are located in large cavities in the network is lower by a factor of 2 in the Ca-bearing glasses. Hence, interaction between cations and $H_2O$ molecules may be weaker in $Ca_{0.5}AlSi_3O_8\cdot 1.3H_2O$. This interpretation is supported by the increase in motional freedom of $H_2O$ molecules with increasing silica content along the line $NaAlSi_3O_8$-$SiO_2$ observed by $^1$H NMR spectroscopy.[17] It should be noted that the dynamic processes detected by neutron scattering are strongly localized, i.e., it is a motion within a cavity of the silicate network. The activation barrier for jumps of water molecules from one cavity to another is much higher in the Ca-bearing glass than in the Na-bearing glass.[20] This trend reflects the compaction of the network topology by incorporation of divalent cations.

## VI. CONCLUSION

The dynamics of water in hydrous aluminosilicate glasses was investigated by quasielastic neutron scattering in the temperature range from 2 K to 420 K. Combination of a backscattering spectrometer with a time-of-flight spectrometer allowed one to investigate the correlation time range from 0.2 ps to 2 ns. The results of elastic scans as well as the temperature dependence of the inelastic spectra $S(Q,t)$ show that the dynamical processes in the Ca glass with 24 mol % water set in at lower temperatures (≈120 K) than in the corresponding Na glass (≈150 K). The shape of the scattering function $S(Q,t)$ indicates a distribution of activation barriers for the dynamics of the water due to the disordered structure of the glasses. In the Ca glass the average activation energy (0.16 eV) is smaller than in the Na glass (0.27 eV) and the (normal) distribution of activation barriers is narrower in the Ca glass ($\sigma_{E_\mathrm{A}}=0.07$ eV) than in the Na glass ($\sigma_{E_\mathrm{A}}=0.11$ eV). The dynamical process is attributed to rotational motion of the water molecules. Rotation of $H_2O$ molecules is faster in the Ca-bearing glass than in the Na-bearing glass though their long-range translational motion is slower.

## ACKNOWLEDGMENT

We are grateful to the Deutsche Forschungsgemeinschaft for financial support.

*Electronic address: indris@pci.uni-hannover.de

†Electronic address: heitjans@pci.uni-hannover.de; URL: http://www.unics.uni-hannover.de/pciheitjans/akhei.html

[1] K. U. Hess and D. B. Dingwell, Am. Mineral. **81**, 1297 (1996).

[2] P. Richet, A. Lejeune, F. Holtz, and J. Roux, Chem. Geol. **128**, 195 (1996).

[3] J. Deubener, R. Müller, H. Behrens, and G. Heide, J. Non-Cryst. Solids **330**, 268 (2003).

[4] E. M. Stolper, Contrib. Mineral. Petrol. **81**, 1 (1982).

[5] M. C. Johnson, A. T. Anderson, Jr., and M. J. Rutherford, Rev. Mineral. **30**, 281 (1994).

[6] G. Heide, M. Leschik, and G. H. Frischat, Geochemistry **61**, 187 (2001).

[7] L. M. Anovitz, J. M. Elam, L. R. Riciputi, and D. R. Cole, J. Archeol. Sci. **26**, 735 (1999).

[8] H. Behrens, C. Romano, M. Nowak, F. Holtz, and D. B. Dingwell, Chem. Geol. **128**, 41 (1996).

[9] H. Behrens, M. Meyer, F. Holtz, D. Benne, and M. Nowak, Chem. Geol. **174**, 275 (2001).

[10] H. Scholze, Naturwissenschaften **47**, 226 (1960).

[11] R. F. Bartholomew and J. W. H. Schreurs, J. Non-Cryst. Solids **38-39**, 679 (1980).

[12] H. Eckert, J. P. Yesinowski, E. M. Stolper, T. R. Stanton, and J. Holloway, J. Non-Cryst. Solids **93**, 93 (1987).

[13] B. C. Schmidt, H. Behrens, T. Riemer, R. Kappes, and R. Dupree, Chem. Geol. **174**, 195 (2001).

[14] L. A. Silver, P. D. Ihinger, and E. M. Stolper, Contrib. Mineral. Petrol. **104**, 142 (1990).

[15] S. Ohlhorst, H. Behrens, and F. Holtz, Chem. Geol. **174**, 5 (2001).

[16] H. Eckert, J. P. Yesinowski, L. A. Silver, and E. M. Stolper, J. Phys. Chem. **92**, 2055 (1988).

[17] B. C. Schmidt, T. Riemer, S. C. Kohn, H. Behrens, and R. Dupree, Geochim. Cosmochim. Acta **64**, 513 (1999).

[18] M. Bée, *Quasielastic Neutron Scattering* (Adam Hilger, Bristol, 1988).

[19] T. Springer and R. E. Lechner, in *Diffusion in Condensed Matter – Methods, Materials, Models*, edited by P. Heitjans and J. Kärger (Springer, Berlin, in press).

[20] H. Behrens and F. Schulze, in *Applied Mineralogy in Research, Economy, Technology and Culture*, edited by D. Rammlmair, J. Mederer, Th. Oberthür, R. B. Heimann, and H. Pentinghaus (Balkema, Rotterdam, 2000), p. 95.

[21] A. C. Withers and H. Behrens, Phys. Chem. Miner. **27**, 119 (1999).

[22] S. Ohlhorst, H. Behrens, F. Holtz, and B. C. Schmidt, in *Applied Mineralogy in Research, Economy, Technology and Culture*, edited by D. Rammlmair, J. Mederer, Th. Oberthür, R. B. Heimann, and H. Pentinghaus (Balkema, Rotterdam, 2000) p. 193.

[23] R. Zorn, B. Frick, and L. J. Fetters, J. Chem. Phys. **116**, 845 (2002).

[24] G. J. Roberts and J. P. Roberts, Phys. Chem. Glasses **7**, 82 (1966).

[25] M. Tomozawa, J. Am. Ceram. Soc. **68**, C251 (1985).

[26] G. J. Wasserburg, J. Geol. **96**, 363 (1988).

[27] M. Helmich and F. Rauch, Glastech. Ber. **66**, 195 (1993).

[28] H. Behrens and M. Nowak, Contrib. Mineral. Petrol. **126**, 377 (1997).

[29] Y. Zhang and H. Behrens, Chem. Geol. **169**, 243 (2000).

[30] R. H. Doremus, in *Reactivity of Solids*, edited by C. W. Mitchell (Wiley, New York, 1969), p. 667.

[31] R. H. Doremus, J. Mater. Res. **10**, 2379 (1995).

[32] Y. Zhang, E. M. Stolper, and G. J. Wasserburg, Geochim. Cosmochim. Acta **55**, 441 (1991).

[33] M. Nowak and H. Behrens, Contrib. Mineral. Petrol. **126**, 365 (1997).

[34] Z. Haider and G. J. Roberts, Glass Technol. **6**, 158 (1970).

[35] H. Behrens, R. Kappes, and P. Heitjans, J. Non-Cryst. Solids **306**, 271 (2002).

[36] V. O. Zavel'sky, N. I. Bezman, and V. A. Zharikov, J. Non-Cryst. Solids **224**, 225 (1998).

[37] In the literature often the term "relaxation time" is used. The motional correlation time is of the order of the mean residence time.